Synthesis and Structural Characterization of Ni^{2+}, Cu^{2+}, Pd^{2+} and Pt^{2+} complexes of 2,2'-(butane-2,3-diylidene)bis(hydrazine-1-carbothioamide)

Fathy A. El-Saied[1], Mayada S. Ali[2], Mohamad M.E. Shakdofa[3,41], Reham M.W. Faried[1], Metwally Madkour[2] Ahmed A. El-Asmy[2,5]

[1]*Chemistry Department, Faculty of Science, El-Menoufia University, Shebin El-Kom, Egypt*

[2]*Chemistry Department, Faculty of Science, Kuwait University, P.O. Box 5969, Safat 13060, Kuwait.*

[3]*Department of Chemistry, college of Science and Arts, Khulais, University of Jeddah, Saudi Arabia*

[4]*Inorganic Chemistry Department, National Research Centre (ID 60014618), 33 El-Bohouth St., P.O. 12622, Dokki, Giza, Egypt*

[5]*Deceased*

Abstract

Ni^{2+}, Cu^{2+}, Pd^{2+} and Pt^{2+} complexes of of 2,2'-(butane-2,3-diylidene)bis(hydrazine-1-carbothioamide) (H_2L) were prepared and fully characterized. The characterization of the prepared compounds were carried out analytically and spectrally using elemental and thermal analyses, FTIR, ^{1}H NMR, ^{13}C NMR, mass and electronic absorption spectra as well as magnetic and molar conductance measurements.The analytical data revesled that the complexes formed in 1:1 molar ratio and all complexes are non-electrolyte. The spectral data showed that the of 2,2'-(butane-2,3-diylidene)bis(hydrazine-1-carbothioamide) (H_2L) behaved as a dibasic tetradentate chelator bonded with the metal ions via thiol sulphur atoms and azomethine nitrogen atoms adopting a square planar geometry for Ni^{2+} , Pd^{2+} and Pt^{2+} complexes, while Cu^{2+} complex adopts a distorted octahedral geometry structure. The thermal analysis showed that the ligand was stable up to 191 ℃ while Ni^{2+}, Pd^{2+} and Pt^{2+} complexes were stable up to temperatures range from 235-320 ℃ and decomposed in one step leading to the formation metal oxide.

Keywords: *Thiosemicarbazone; metal complexes, Electronic spectrum, NMR, IR*

1. Introduction

The metal complexes for the compounds incorporating nitrogen and sulfur atoms have been attracted numerous researchers attention because of their important and effective role in different fields.[1-5] Among them, thiosemicarbazone compounds of formula ($R^1R^2C^2=N^3$-$N^2(H)$-$C^1(=S)N^1R^3R^4$) which represent an important class of S/N-thio-ligand due to their biological and catalytic activities [6-12]. The activity of these thio-ligand can be interrelated to their chelation ability toward the ions of transition elements. The complexes of thiosemicarbazone have several applications such as anti-cancer,[13-17] anti-HIV, anti-viral, [18, 19] anti-fungal, anti-bacterial, antimicrobial, anti-molluscicide.[20-25] anti-tumor,[26] Anti-neurotoxic,[27] anti-proliferation,[28] and anti-tubercular,[29] anti-inflammatory.[30] Ni^{2+} and Co^{3+} complexes of thiosemicarbazone ligands incorporating N-heterocyclic moiety possess a DNA binding ability and cleavage activity as well as an inhibitory effect on the topoisomerase I/II.[31, 32] While Cu^{2+} complexes of thiosemicarbazone act as models for galactose oxidase especially its redox reactions at a biological level[33] and Mo_2^{2+}complexes of S-methyl-5-bromosalicylidene-Nalkyl substituted thiosemicarbazone

[1] Corresponding author Prof. Mohamad M. E. Shakdofa, mshakdofa@gmail.com

ligands showed antioxidant and catalase-inhibitory activities.[34] The complexes of thiosemicarbazone were also used as precursors for preparation of metal oxide nanoparticles.[35, 36] Because of their optoelectronic characteristics, the role of metal oxide nanoparticles in water treatment from organic colorants via photocatalysis technique has acquired a great benefit.[37] This article devoted to the preparation of Ni^{2+}, Cu^{2+}, Pd^{2+} and Pt^{2+} complexes of of 2,2'-(butane-2,3-diylidene)bis(hydrazine-1-carbothioamide) (H_2L). The geometrical and structural charateristics of the prepared thiosemicarbazone and its complexes were characterized using spectral and thermal techniques such as Elemental and thermal analyses, FTIR, ^{1}H NMR, ^{13}C NMR, mass and electronic absorption spectra as well as magnetic and molar conductance measurements.

2. Experimental

2.1. Instrumentation and measurements

Elemental analyses (C, H, N) were performed at RSP Unit of Kuwait University. TGA was carried out on a Shimadzu TGA-60 thermal analyzer (30-850 °C) at a heating rate of 10 °C/min. Molar conductance was measured in DMSO using a Bibby conductometer type MC-1. IR spectra were performed on a FTIR-6300 type A (400-4000 cm^{-1}). The electronic spectra were performed on Cary 5 UV-Vis Spectrophotometer. The ^{1}H NMR (600 MHz) and ^{13}C NMR (150 MHz) spectra of the ligand and its Pd^{2+}, Pt^{2+} complexes were recorded in DMSO-d_6 using Brucker WP 200 SY spectrometer (600 MHz). Chemical shifts (δ) were reported in ppm using TMS as the internal standard. Mass spectra were studied using a GC-MS Thermo-DFS (BG-FAB) mass spectrometer. Magnetic susceptibilities were measured by a Johnson-Matthey magnetic balance using $Hg[Co(CNS)_4]$ as a calibrating agent. Diamagnetic corrections were made using Pascal's constants.[38] The magnetic moments were calculated from the equation: $\mu_{eff}=2.84(\chi_M^{corr}T)^{1/2}$.

2.2. Synthesis of the ligand

The ligand adding 30 mL hot ethanol solution of thiosemicarbazide (18.12 g, 0.2 mol) slowly to 30 mL hot ethanollic solution of 2,3-butandione (23.2 g, 0.1 mol)(Scheme 5) then heating these mixtures under reflux, with continuous stirring, in a heating mantle for 2h. The precipitate was collected by filtration, washed with ethanol, diethyl ether and finally dried under vacuum over silica gel to afford the corresponding thiosemicarbazone (**H_2L, 1**) **(Fig. 1)**. Yield: 77%; m.p.: 225 ^oC. Elemental analysis for $C_6H_{12}N_6S_2$ (m/z 232.32): calcd (Found) %C 32.02 (31.04), %H 5.21 (5.16), %N 36.17 (36.07), %S 27.60 (27.83). IR (KBr, cm^{-1}), 3408, 3248, 3194, 3149 ν(NH/NH_2), 1594 ν(C=N), 948 ν(N-N), 833 ν(C=S). ^{1}H-NMR (600 MHz, DMSO-d_6): δ (ppm) = 11.061, 10.197 (s, 2 H, $NH^{6\&7}$), 8.390, 8.101 (s, 4H, $NH_2^{10\&12}$), 1.947 (s, 6H, $CH_3^{3\&14}$), ^{13}C-NMR (150 MHz, DMSO-d_6): 183.12 (C8&9), 148.37 (C1&2), 13.81 (C3), 11.55 (C14). UV. Vis. 1 cm quartz cells, (DMSO) 275, 327, 365, 377, 395 nm.

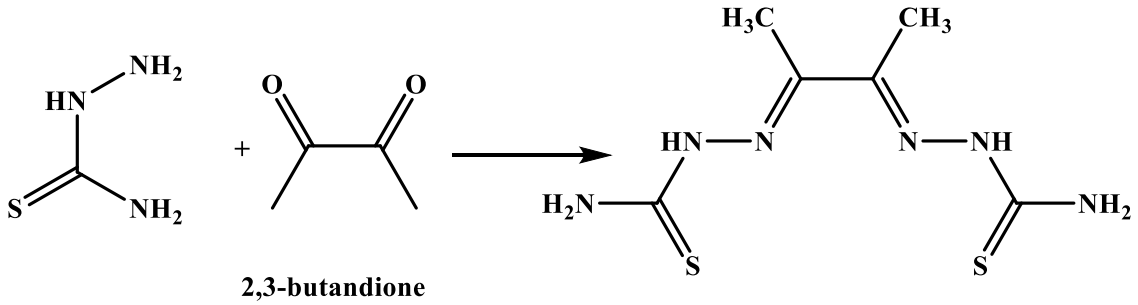

2,3-butandione

2,2'-(butane-2,3-diylidene)bis(hydrazine-1 -carbothioamide)

Fig. 1: Synthesis of 2,2'-(butane-2,3-diylidene)bis(hydrazine-1-carbothioamide) (H_2L, 1)

2.3. Synthesis of the complexes

2.3.1. Synthesis of the binuclear Ni^{2+} (2) and Cu^{2+} complexes (5)

The **Ni^{2+} and Cu^{2+}** complexes [were prepared by heating a mixture of the ligand (223 mg, 1 mmol) and $Ni(OAc)_2.4H_2O$ or $Cu(ClO_4)_2.6H_2O$ (1 mmol) in 30 ml ethanol solution for 4-6 h. The precipitate was collected by filtration, washed with ethanol, diethyl ether and finally dried under vacuum over silica gel.

Ni^{2+}-Complex (2): Yield: 67%, m.p. >300 ^oC; color: dark brown; μ_{eff} = Dia.; molar conductivity (Λ_m): 4.34 $\Omega^{-1}cm^2mol^{-1}$, Elemental analysis for [Ni(L)], $C_6H_{10}N_6S_2Ni$, (m/z 289.00): Calcd. (Found) %C 24.94 (25.06), %H 3.49 (3.44), %N 29.08 (28.79), %S 22.19 (22.46) %Ni 20.31 (19.98). IR (KBr, cm^{-1}), 3410, 3290, 3225, 3147 $\nu(NH_2)$, 1582, 1630 ν(C=N), 1008 ν(N-N), 716 ν(C=S). 497 ν(Ni←N), 451 ν(Ni-S). UV. Vis. 1 cm quartz cells, DMSO) 258, 300, 335, 395, 450, 600, 670 nm.

Cu^{2+}-Complex (5): Yield: 59%, m.p. >300 ^oC; color: dark brown; μ_{eff} = 1.80.; molar conductivity (Λ_m): 8.66 $\Omega^{-1}cm^2mol^{-1}$, Elemental analysis for $[Cu(L)(H_2O)_2]$, $C_6H_{14}N_6S_2O_2Cu$, (m/z 329.88): Calcd. (Found) %C 21.85 (22.17), %H 4.28 (4.14), %N 25.48 (25.08), %S 19.44 (19.52) %Cu 19.26 (18.95). IR (KBr, cm^{-1}), 3411, 3350, 3293, 3258 3154 $\nu(NH_2/H_2O)$, 1588, 1629 ν(C=N), 1000 ν(N-N), 697 ν(C=S). 519 ν(Cu←N), 460 ν(Cu-S). UV. Vis. 1 cm quartz cells, DMSO) 255, 310, 340, 475, 610 nm.

2.3.2. Synthesis of the Pd^{2+} and Pt^{2+}complexes (3) and (4)

Pd^{2+} and Pt^{2+}complexes were prepared by heating a mixture of the ligand (223 mg, 1 mmol) and K_2PdCl_4 or K_2PtCl_4 (1 mmol) in 30 ml aqueous ethanol (v/v) on a water bath for 5 h. The precipitate was collected by filtration, washed with hot distilled water followed by ethanol, diethyl ether and finally dried under vacuum over silica gel.

Pd^{2+}-Complex (3): Yield: 50%, m.p. >300 ^oC; color: violet; μ_{eff} = Dia.; molar conductivity (Λ_m): 5.83 $\Omega^{-1}cm^2mol^{-1}$, Elemental analysis for [Pd(L)], $C_6H_{10}N_6S_2Pd$, (m/z 336.37): Calcd. (Found) %C 21.40 (20.98), %H 2.99 (2.91), %N 24.96(24.84), %S 19.04 (18.86) %Pd 31.60 (31.28 IR (KBr, cm^{-1}), 3401, 3289, 3142 $\nu(NH_2)$, 1564, 1629 ν(C=N), 1008 ν(N-N), 712 ν(C=S), 519 ν(Pd←N), 476 ν(Pd-S). ^{1}H-NMR (600 MHz, DMSO-d_6): δ (ppm) = 7.614 (s, 4H, $NH_2^{10\&12}$), 1.972 (s, 6H, $CH_3^{3\&14}$), ^{13}C-NMR (150 MHz, DMSO-d_6): 180.21 (C8&9), 156.37 (C1&2), 13.81 (C3&14). UV. Vis. 1 cm quartz cells, DMSO) 257, 332, 395, 410, 485, 575, 610 nm.

Pt^{2+}-Complex (4): Yield: 67%, m.p. >300 ^oC; color: olive; μ_{eff} = Dia.; molar conductivity (Λ_m): 21.52 $\Omega^{-1}cm^2mol^{-1}$, Elemental analysis for [Pt(L)], $C_6H_{10}N_6S_2Pt$, (m/z 425.39): Calcd. (Found) %C 16.94 (16.56), %H 2.37 (2.45), %N 19.76 (19.25), %S 15.07 (15.36) %Pt 45.86 (45.41). IR (KBr, cm^{-1}), 3408, 3249, 3193, 3149 $\nu(NH_2)$, 1590, 1630 ν(C=N), 1005 ν(N-N), 713 ν(C=S). 497 ν(Pt←N), 451 ν(Pt-S). ^{1}H-NMR (600 MHz, DMSO-d_6): δ (ppm) = 7.833 (s, 4H, $NH_2^{10\&12}$), 1.954 (s, 6H, $CH_3^{3\&14}$), ^{13}C-NMR (150 MHz, DMSO-d_6): 178.89 (C8&9), 157.61 (C1&2), 13.89 (C3&14). UV. Vis. 1 cm quartz cells, DMSO) 275, 325, 355, 375, 397, 640 nm.

3. Results and discussion

The obtained ligand and its complexes **(1-5)** are air stable. The complexes possess assorted colors, the solubility test illustrates that the complexes showed that these complexes are water insoluble and soluble in polar aprotic solvent like DMSO and DMF. The value of molar conductivity of complexes **(2-5)** are 4.34, 5.83, 21.52 and 8.66 $\Omega^{-1}cm^2mol^{-1}$ respectively indicating their non-electrolytic nature.[39] The scientifically high value for Pt^{2+}

complex could be due to the partial solvolysis by DMSO.[39, 40] The elemental, thermal, molar conductivity, magnetic moment measurements, spectral analyses as well as X-ray single crystal data are located in experimental section and Table 1. The data illustrated that all complexes were composed in molar ratio (1L:1M) with formulae $[M(L)(X_2)]$ where M=Ni^{2+}, Pd^{2+} or Pt^{2+} and X = 0 but when, M= Cu^{2+}, X = H_2O as shown in (Fig. 2).

$[ML^5)(X_2)]$
M= Ni(II), X= 0 (22)
M=Pd(II),X= 0 (23)
M=Pt(II), X= 0 (24)
Cu(II), X= H_2O (25)

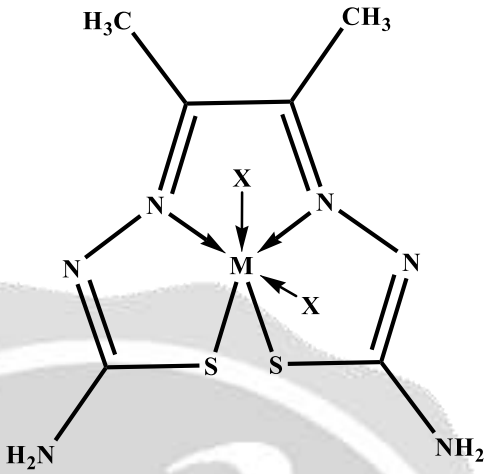

Fig.2: Structure representation of Ni^{2+}, Pd^{2+}, Pt^{2+} and Cu^{2+} (2-5)

3.1. NMR spectrum

3.1.1. ^{1}H-NMR spectrum

The ligand ^{1}H-NMR spectrum in DMSO-d_6 (Fig. 3) agree with the proposed structure. The two chemical shifts noted as singlet at 11.061 and 10.197 ppm (s, 1H, NH^6) and (t, 1H, NH^7); While the doublet chemical shifts noted at 8.390 (dd, 2H, $^{10}H_2N$) and 8.101(d, 2H, $^{12}H_2N$). The spectrum also showed chemical shifts at δ = 1.947 ppm for CH_3 group at position (3 & 14) were imputed to the methyl group protons. ^{1}H-NMR spectrum clarifies, that the thiosemicarbazone **(1)** offered only a thio-keto form; there's no evidence for existence of the thio-enol form. This conclusion was supported by the existence of chemical shifts relevant to (NH) and the complete lack of a chemical shift relevant to (SH) of the thio-enol form.[28] The ^{1}H NMR spectra of the Pd^{2+} and Pt^{2+}complexes showed that the thio-amide protons are disappeared clarifying that the Pd^{2+} and Pt^{2+} are bonded to the thio-enol tautomer via the deprotonated thio-amide sulfur atom.

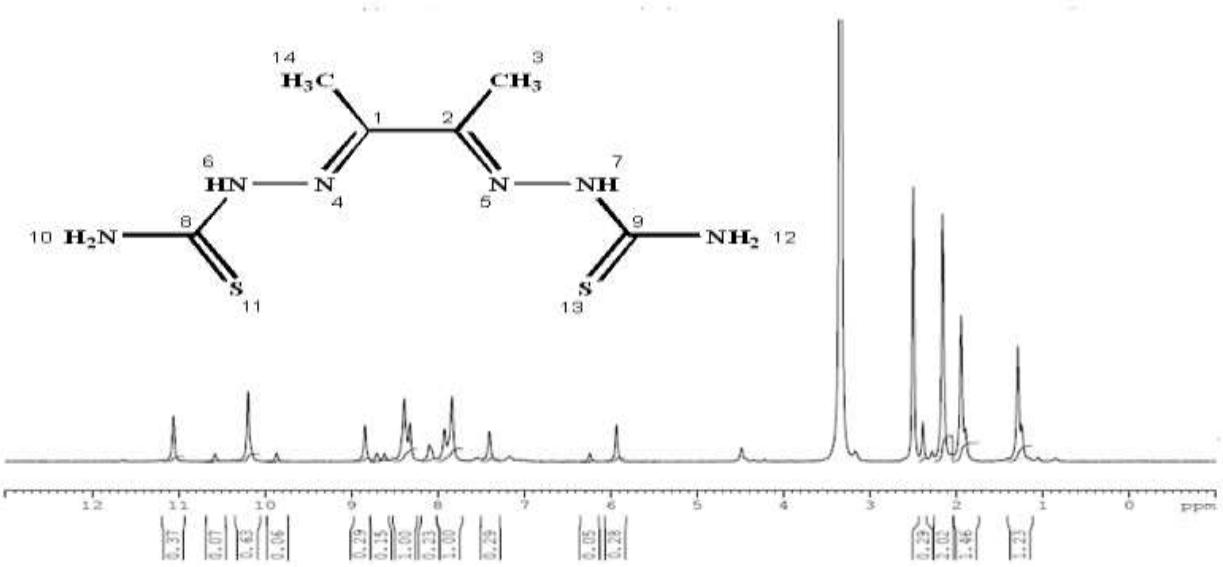

Fig. 3: ^{1}HNMR spectrum of thiosemicarbazone (H_2L, 1)

3.1.2. ^{13}C- NMR spectrum

The ^{13}C-NMR spectrum of thiosemicarbazone **(1)** (Fig. 4) displayed a chemical shift at 183.12 ppm assigning to the thioketone carbon atom (^{8,9}C=S).[41, 42] The imine carbon (^{1,2}C=N) chemical shift was appeared at 148.37 ppm.[41, 42] The peaks appearing at 11.55, 13.81 ppm can be related the methyl group carbon atoms ($^{3,14}CH_3$). For Pd^{2+} and Pt^{2+}complexes the thio-amide δ(C=S) signal shift to upfield by about 5, 3 ppm in comparing with the parent thiosemicarbazone. This upfield shift may be due to the movement of electron density from the thio-amide moiety to the Pd^{2+} and Pt^{2+} ions upon chelation that could have caused the thio-amide carbon nuclei to be deshielded hence the upfield shift.[14]

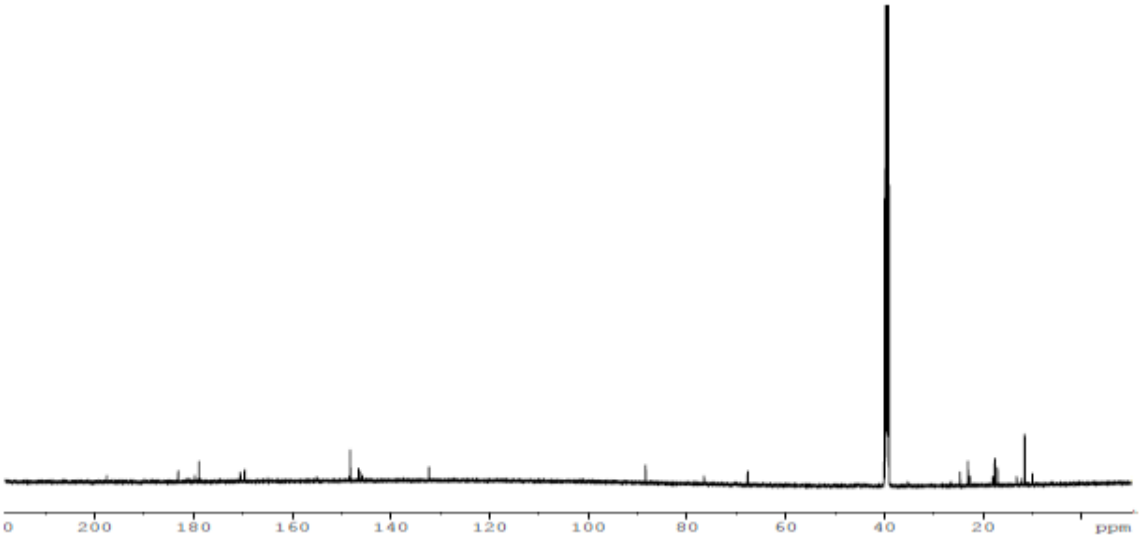

Fig. 4: ^{13}CNMR spectrum of thiosemicarbazone (H_2L, 1)

3.2. Mass spectrum (MS)

The MS of the thiosemicarbazone **(1)** (Fig. 5) showed a molecular peak at m/z = 232.1 (7%) and weak peaks surround it due to ^{13}C and ^{15}N isotopes. The other positive ions give peaks at 215.1 (15%), 174.2 (3%), 116.0 (100%), 86.1 (6%) and 56.07 (32%) mass numbers. The intensities of these peaks indicate the stabilities of these fragments. The MS of [Ni(L)] displayed multi peaks representing sequential degradation for the molecule. The peak appeared at m/e = 2 (Calcd. 289.0) representing the stable species [Ni(L)] with 15% abundance. Also, there are peaks at 274, 259, 245 and 231 mass numbers due to the removal of methyl and amino groups. The other positive ions give peaks at mass numbers 200, 193.0 172, 145, 130, 113 and mass numbers representing sequential degradation for the molecule. The spectrum of [Pd(L)] The peak appeared at m/e = 337 (Calcd. 336.73) representing the stable species [Pd(L^5)] with 8% abundance. The peaks at 323, 309, 293, 278 is corresponding the removal of methyl and amino groups. The mass spectrum of [Pd(L)] showed a weak molecular ion peaks at 247, 216, 191, 135 representing sequential degradation for the molecule. The mass spectrum of Pt^{2+} complex showed peak at 425 (calcd. 425.39) representing the molecular ion peak for the species [Pd(L)]. The peaks at 411, 397, 382, 367 is corresponding the removal of methyl and amino groups. The mass spectrum of [Pt(L)] showed a weak molecular ion peaks at 336, 309, 281, 266, 251, 224 representing sequential degradation for the molecule. On the other hand, the MS of [Cu(L)].2H_2O showed a peak of intensity 60% at e/m = 293.1 corresponding exactly [Cu(L)]. This species may be formed after the removal of 2H_2O. The positive ions peaks at 235 (2%) may be due to the removal of methyl and amino groups. The other positive ions give peaks at mass numbers 192 (4%), 178.0 (1%) and 164 (65%), 141 (13%), 124 (16%) mass numbers representing sequential degradation for the molecule.

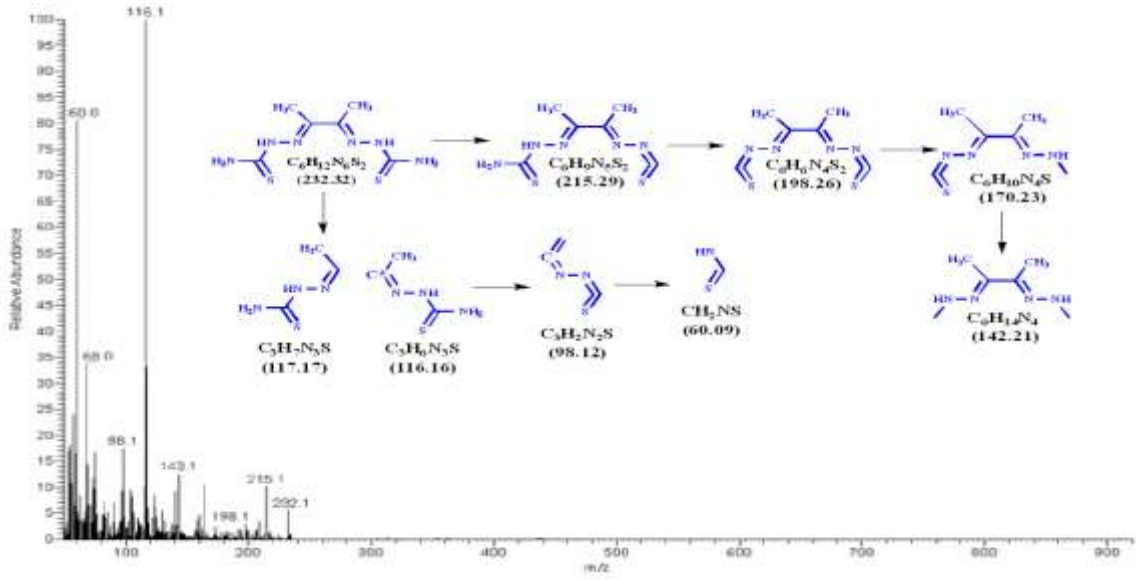

Fig. 5: Mass spectrum of thiosemicarbazone (H_2L, 1)

3.3. Infrared spectrum (IR)

The IR bands of the thiosemicarbazone **(1)** spectrum shows peaks at 3408, 3248 and 3194, 3149 cm^{-1} which could be attributed to the imine ν(N-H) and ν(NH_2).[9, 43, 44] The weak bands which appeared at 3000, 2950, 2990 cm^{-1} could be attributed to the azomethine and aliphatic protons.[45, 46] The spectrum also displayed bands at 1594 and 833 cm^{-1} which they are owing to imine ν(C=N) group, and thio-amide ν(C=S)[47, 48] groups respectively. These observations referee that, the thiosemicarbazone **(1)** adopted only a thio-keto form in the solid state. This conclusion is endorsed by the absence of the band related to the ν(S–H) linkage (generally shows in the 2500–2600 cm^{-1}).[47, 49-51] The coordination manner can be obvious by matching the complexes IR spectra with the IR spectrum of thiosemicarbazone **(1)**. The matching clarifies that the thiosemicarbazone **(1)** worked as **Dibasic bi-dentate** bonded with the Ni^{2+}, Pd^{2+}, Pt^{2+} and Cu^{2+} ions via the imine nitrogen atom, thio-amide group in its thio-enol form in complexes **(2-5)**. This way of chelation was mended by four proofs as follow:

i.The negative shift in position (4-30 cm^{-1}) and intensity of the band of imine group C=N).[22, 42]

ii.The misplaced of the imine group ν(N-$H^{6,7}$) band upon chelation, signifying that the thiosemicarbazone in these complexes interacted in the thio-enol form, that was endorsed by the appearing of new band in the region 1629-1630 cm^{-1}, assignable to ν(C=N-N=C).[42]

iii.The negative shift in position (121-136 cm^{-1}) and intensity of the ν(C=S) group which appears in the range 697-716 cm^{-1}.[13, 36, 48, 52]

iv.The being of new bands at 451-476 and 497-519 cm^{-1} could be attributed to the ν(M-S) and ν(M←N) consecutively.[22, 53]

3.4. Magnetic moment

The μ_{eff} data of complexes **(2-5)** at 300 °K are depicted in (Table 32). The μ_{eff} results demonstrated that Ni^{2+}, Pd^{2+} and Pt^{2+} are diamagnetic which confirmed that these complexes have a square planar geometry. While the μ_{eff} for Cu^{2+}complex was found to be equal to 1.80 BM.

3.5. Electronic absorption spectrum (EA)

The EA spectra of the thiosemicarbazone **(1)** and its complexes were measured at 300 °K in DMSO and outlined in Table 32. The EA absorption data of thiosemicarbazone **(1)** (Fig. 6) showed five bands at 275, 327,

365, 377, 395 nm. The band at 275 nm can be ascribed to the $\pi\rightarrow\pi^*$ intra-ligand transitions[54-56] which nearly unchanged on chelation. Whereas the bands at 327 and 365 nm can be returned to $n\rightarrow\pi^*$ of the (C=N) azomethine and (C=S) thio-amide groups.[28, 55] The shifting of these bands in complexes spectra demonstrating their involvement in chelation with center cations. While the bands at 377 and 395 nm could be imputed to $\pi\rightarrow\pi^*$ transition relating to the azomethine and thio-amide chromophore.[22, 54] In some complexes, new bands were observed in the 400-475 nm ranges may be attributed to LMCT transitions. The EA spectrum of diamagnetic Ni^{2+} complex **(2)** in DMSO (Fig 7) showed three bands at 450, 600 and 670 nm. which may be attributed to the $^1A_{1g}\rightarrow{}^1A_{2g}$, $^1A_{1g}\rightarrow{}^1B_{1g}$ and $^1A_{1g}\rightarrow{}^1E_{1g}$ transitions.[57, 58] The first band could be attributed to charge transfer transition overlapped with $^1A_{1g}\rightarrow{}^1E_g$ transition while the second and third bands could be assigned to the $^1A_{1g}\rightarrow{}^1B_{1g}$ and $^1A_{1g}\rightarrow{}^1E_{1g}$ transitions which is supporting the square-planar geometry of Ni^{2+} complex that is agreeable with diamagnetic nature of this complex. The square planar Pd^{2+} complexes showed three spin-allowed transitions, $^1A_{1g}\rightarrow{}^1A_{2g}$, $^1A_{1g}\rightarrow{}^1B_{1g}$ and $^1A_{1g}\rightarrow{}^1E_{1g}$ as expected for D4h symmetry. The d orbitals split into empty B_{1g} (d_{x2-y2}) orbital located at higher energy level than the occupying orbitals A_{1g} (d_{z2}), B_{2g} (d_{xy}), E_g (d_{xz}, d_{yz}).[57, 59] The EA spectrum of Pd^{2+} complex **(3)** (Fig. 8) showed three bands at 600, 575 and 485 nm which are attributable to the transitions $^1A_{1g}\rightarrow{}^1A_{2g}$, $^1A_{1g}\rightarrow{}^1B_{1g}$ and $^1A_{1g}\rightarrow{}^1E_{1g}$ indicating to a square planar geometry around the Pd^{2+} ion which is agreeable with diamagnetic nature of this complex.[9, 60, 61] In square planar Pt^{2+} complexes three d-d spin-allowed transitions are expected corresponding to the transitions from the three lower-lying ''d'' levels to the empty d_{x2-y2} orbital. The ground state is $^1A_{2g}$ and the excited states corresponding to these transitions are $^1A_{2g}$, $^1B_{1g}$ and ^1E_g in increasing order of energy.[57, 62] The EA spectrum of Pt^{2+} complex **(4)** (Fig. 8) showed two bands at 397 and 640 nm. The first band could be attributed to charge transfer transition overlapped with $^1A_{1g}\rightarrow{}^1E_g$ transition while the second band which is very broad could be assigned to the transition $^1A_{1g}\rightarrow{}^1A_{2g}$, overlapped with $^1A_{1g}\rightarrow{}^1B_{1g}$ transition which is supporting the square-planar geometry of Pt^{2+} complex that is agreeable with diamagnetic nature of this complex.[57, 63-66] The EA spectrum of Cu^{2+} complex **(5)** (Fig. 9) displayed a single wide band at 610 nm which may be attributed to the super-imposed of the transition $^2B_{1g}\rightarrow{}^2E_g(d_{xz-yz}\leftarrow d_{x2-y2})$, $^2B_{1g}\rightarrow{}^2A_{1g}(d_{z2}\leftarrow d_{x2-y2})$, $^2B_{1g}\rightarrow{}^2B_{2g}(d_{xy}\leftarrow d_{x2-y2})$ suggesting a distorted octahedral geometry around the Cu^{2+} centers.[57, 67, 68]

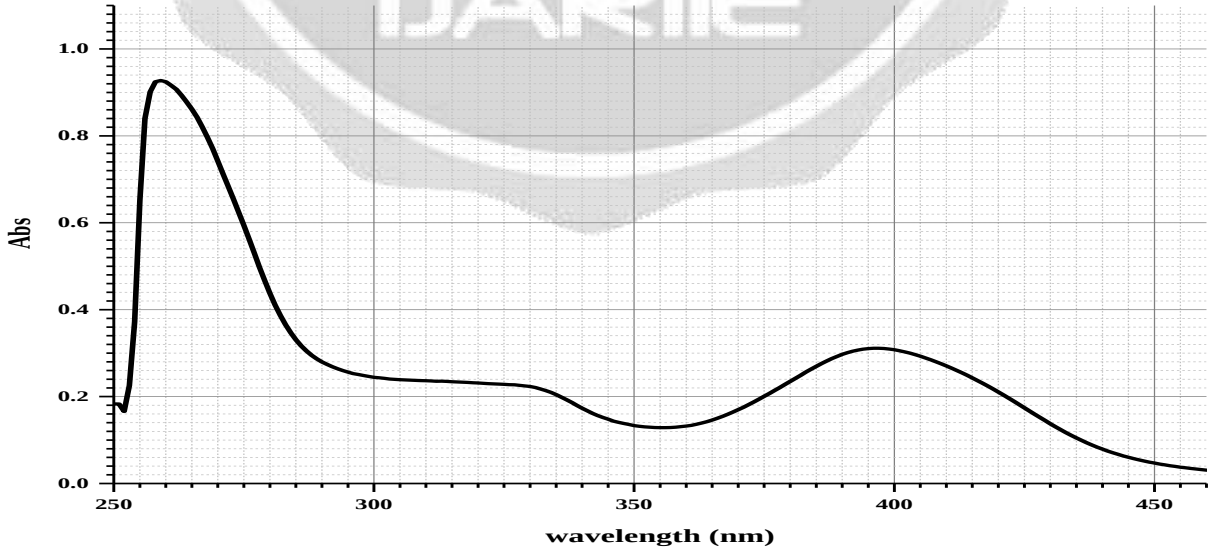

Fig. 6: Electronic absorption spectrum of the ligand (H_2L, 1)

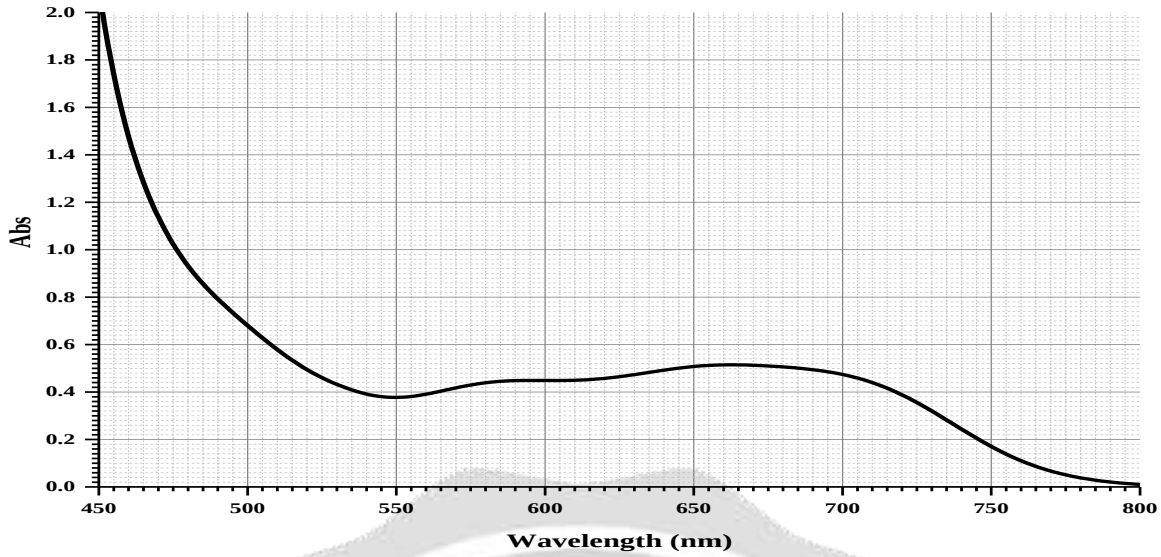

Fig. 7: Electronic absorption spectrum of the Ni^{2+} complex (2)

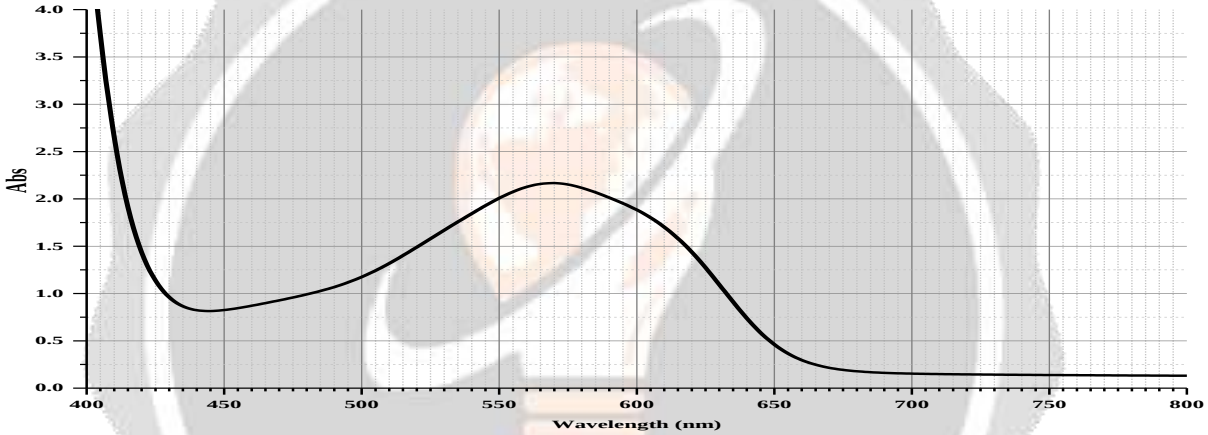

Fig. 8: Electronic absorption spectrum of the Pd^{2+} complex (3)

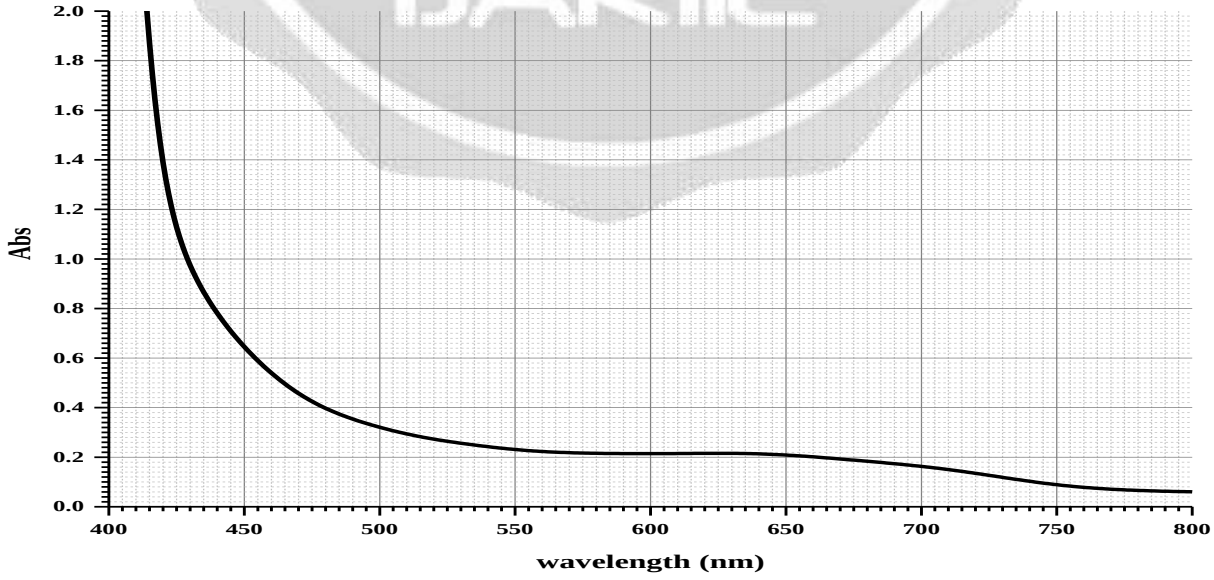

Fig. 9: Electronic absorption spectrum of Pt^{2+} complex (4)

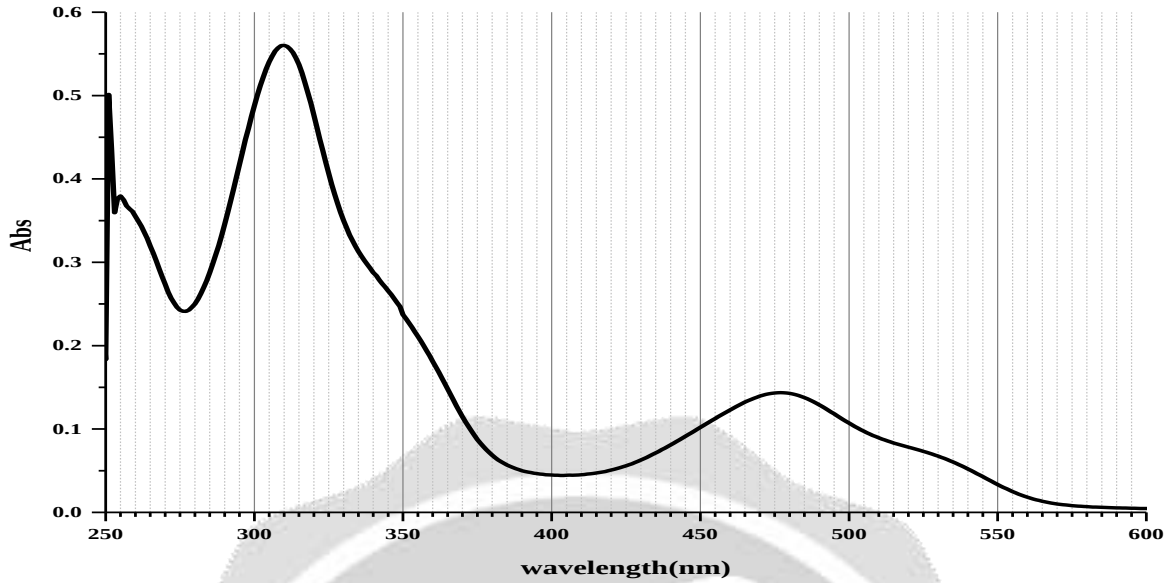

Fig. 10: Electronic absorption spectrum of Cu^{2+} complex (5)

III.1.7. Thermal analysis

To achieve further information about the stabilization of the prepared compounds **(1-4)**. The thermo-gravimetric analysis measured in the 25 to 800 °C range. The data of thermo-gravimetric are outlined in (Table 1) and proved that there is an obvious matching in the losing weight between the suggested and calculated formulae. All complexes displayed a steady part till 200 ^{o}C refereeing lack of any solvent abroad the coordination sphere. The TG thermograms of compounds are denoted that the **(1-4)** showed that the ligand is stable up to 191 and losing amino group at 191-221 °C consequentially decomposed completely in the temperature range 230-650°C with weight loss 91.67 % (calcd. 93.10%). While Ni^{2+}, Pd^{2+} and Pt^{2+} complexes decomposed in one step within temperature ranged from 235 to 800 °C with weight loss equal to 74.59, 64.17 and 51.66 % (calcd. 74.16, 64.83% and 51.32%) leaving NiO, Pd+C and Pt+C.

Table 1. Thermogravimetric data of thiosemicarbazone (1) and its complexes (2-4)

No	Temp. (°C)	Weight loss (%) Found (calcd.)	**assignment**
(1)	30-191	-	Stable
	191-221	7.38(6.90)	Elimination of NH_2
	230-650	91.67 (93.10)	Complete decomposition of the ligand
(2)	30-275	--	Stable
	275-800	74.59(74.16)	decomposition of the complex
	800	25.40(25.84)	NiO formed
(3)	30-320	--	Stable
	320-406	64.17(64.83)	Complete decomposition of the complex
	406	35.83(35.17)	Pd+C formed
(4)	30-235	--	Stable
	235-396	51.66(51.32)	Complete decomposition of the complex
	396	48.33(48.68)	Pt+C formed

3. Conclusion

Ni^{2+}, Cu^{2+}, Pd^{2+} and Pt^{2+} complexes of of 2,2'-(butane-2,3-diylidene)bis(hydrazine-1-carbothioamide) (H_2L) have been prepared and characterized by analytical and spectral techniques such as elemental and thermal analysis, IR, NMR, Mass and electronic spectra as well as magnetic and molar conductance measurements. The result of analyses revealed that ligand acted as dibasic tetradentate chelator bonded to metal ions via the thiol sulpher atoms and azometnime nitrogen atoms given a square planar geometry for the Ni^{2+} , Pd^{2+} and Pt^{2+} while for Cu^{2+} give a distorted octahedral geometry. The thermal analysis demonstrated that all complexes were stable in the temperature range 30-320 °C and decomposed in one step ended with the formation metal oxide or the metal with carbon.

Reference

1. M. M. E. Shakdofa, A. A. Labib, N. A. Abdel-Hafez, H. A. Mousa, *Appl. Organomet. Chem.* **2018**, *32*, e4581.
2. A. A. El-Asmy, O. A. El-Gammal, H. S. Saleh, *Spectrochim. Acta Part A Mol. Biomol. Spectrosc.* **2008**, *71*, 39.
3. A. A. El-Asmy, N. M. El-Metwally, G. A. Al-Hazmi, *Transition Met. Chem.* **2006**, *31*, 673.
4. S. A. Hosseini-Yazdi, P. Samadzadeh-Aghdam, R. Ghadari, *Polyhedron* **2018**, *151*, 221.
5. M. Huseynova, P. Taslimi, A. Medjidov, V. Farzaliyev, M. Aliyeva, G. Gondolova, O. Şahin, B. Yalçın, A. Sujayev, E. B. Orman, A. R. Özkaya, İ. Gulçin, *Polyhedron* **2018**, *155*, 25.
6. E. S. A. El-Samanody, S. A. AbouEl-Enein, E. M. Emara, *Appl. Organomet. Chem.* **2018**, *32*.
7. E.-S. A. El-Samanody, M. W. Polis, E. M. Emara, *J. Mol. Struct.* **2017**, *1144*, 300.
8. E.-S. A. El-Samanody, S. M. Emam, E. M. Emara, *J. Mol. Struct.* **2017**, *1146*, 868.
9. A. K. El-Sawaf, F. El-Essawy, A. A. Nassar, E.-S. A. El-Samanody, *J. Mol. Struct.* **2018**, *1157*, 381.
10. C. Balachandran, J. Haribabu, K. Jeyalakshmi, N. S. P. Bhuvanesh, R. Karvembu, N. Emi, S. Awale, *J. Inorg. Biochem.* **2018**, *182*, 208.
11. S. Roy, Saswati, S. Lima, S. Dhaka, M. R. Maurya, R. Acharyya, C. Eagle, R. Dinda, *Inorg. Chim. Acta* **2018**, *474*, 134.
12. Saswati, M. Mohanty, A. Banerjee, S. Biswal, A. Horn, G. Schenk, K. Brzezinski, E. Sinn, H. Reuter, R. Dinda, *J. Inorg. Biochem.* **2020**, *203*, 110908.
13. B. Şen, H. K. Kalhan, V. Demir, E. E. Güler, H. A. Kayalı, E. Subaşı, *Mater. Sci. Eng. C* **2019**, *98*, 550.
14. F. P. Andrew, P. A. Ajibade, *J. Mol. Struct.* **2018**, *1170*, 24.
15. F.-U. Rahman, A. Ali, H.-Q. Duong, I. U. Khan, M. Z. Bhatti, Z.-T. Li, H. Wang, D.-W. Zhang, *Eur. J. Med. Chem.* **2019**, *164*, 546.
16. W. Cao, J. Qi, K. Qian, L. Tian, Z. Cheng, Y. Wang, *J. Inorg. Biochem.* **2019**, *191*, 174.
17. S. Kallus, L. Uhlik, S. van Schoonhoven, K. Pelivan, W. Berger, É. A. Enyedy, T. Hofmann, P. Heffeter, C. R. Kowol, B. K. Keppler, *J. Inorg. Biochem.* **2019**, *190*, 85.
18. A. Karaküçük-İyidoğan, D. Taşdemir, E. E. Oruç-Emre, J. Balzarini, *Eur. J. Med. Chem.* **2011**, *46*, 5616.
19. M. C. Soraires Santacruz, M. Fabiani, E. F. Castro, L. V. Cavallaro, L. M. Finkielsztein, *Bioorg. Med. Chem.* **2017**, *25*, 4055.
20. A. M. El-Seidy, M. M. Shakdofa, H. A. Mousaa, *Research Journal of Pharmaceutical, Biological and Chemical Sciences* **2017**, *8*, 573.
21. Mohamad M. E. Shakdofa, A. S. El-tabl, A. S. Al-hakimi, M. A. Wahba, N. Morsy, *Ponte* **2017**, *73*, 52.
22. A. Akbari, H. Ghateazadeh, R. Takjoo, B. Sadeghi-Nejad, M. Mehrvar, J. T. Mague, *J. Mol. Struct.* **2019**, *1181*, 287.
23. A. B. M. Ibrahim, M. K. Farh, P. Mayer, *Inorg. Chem. Commun.* **2018**, *94*, 127.
24. A. B. M. Ibrahim, M. K. Farh, S. A. El-Gyar, M. A. El-Gahami, D. M. Fouad, F. Silva, I. C. Santos, A. Paulo, *Inorg. Chem. Commun.* **2018**, *96*, 194.
25. E. Shahsavani, A. D. Khalaji, N. Feizi, M. Kučeráková, M. Dušek, *Inorg. Chim. Acta* **2015**, *429*, 61.
26. T. E. Kokina, L. A. Glinskaya, L. A. Sheludyakova, Y. A. Eremina, L. S. Klyushova, V. Y. Komarov, D. A. Piryazev, A. V. Tkachev, S. V. Larionov, *Polyhedron* **2019**, *163*, 121.
27. F. A. El-Saied, T. A. Salem, M. M. E. Shakdofa, A. N. Al-Hakimi, *Appl. Organomet. Chem.* **2018**, *32*, e4215.

28. M. M. E. Shakdofa, H. A. Mousa, A. M. A. Elseidy, A. A. Labib, M. M. Ali, A. S. Abd-El-All, *Appl. Organomet. Chem.* **2018**, *32*, e3936.
29. A. Kotian, K. Kumara, V. Kamat, K. Naik, D. G. Kokare, A. Nevrekar, N. K. Lokanath, V. K. Revankar, *J. Mol. Struct.* **2018**, *1156*, 115.
30. S. Saranya, J. Haribabu, V. N. Vadakkedathu Palakkeezhillam, P. Jerome, K. Gomathi, K. K. Rao, V. H. Hara Surendra Babu, R. Karvembu, D. Gayathri, *J. Mol. Struct.* **2019**, *1198*, 126904.
31. J. Deng, T. Li, G. Su, Q.-P. Qin, Y. Liu, Y. Gou, *J. Mol. Struct.* **2018**, *1167*, 33.
32. J. Deng, G. Su, P. Chen, Y. Du, Y. Gou, Y. Liu, *Inorg. Chim. Acta* **2018**, *471*, 194.
33. R. Llanguri, J. J. Morris, W. C. Stanley, E. T. Bell-Loncella, M. Turner, W. J. Boyko, C. A. Bessel, *Inorg. Chim. Acta* **2001**, *315*, 53.
34. S. Eğlence, M. Şahin, M. Özyürek, R. Apak, B. Ülküseven, *Inorg. Chim. Acta* **2018**, *469*, 495.
35. E.-S. A. El-Samanody, A. K. El-Sawaf, M. Madkour, *Inorg. Chim. Acta* **2019**, *487*, 307.
36. Z. Piri, Z. Moradi–Shoeili, A. Assoud, *Inorg. Chim. Acta* **2019**, *484*, 338.
37. M. Anjum, R. Miandad, M. Waqas, F. Gehany, M. A. Barakat, *Arab. J. Chem.* **2016**.
38. L. Lewis, R. G. Wilkins, 'Modern Coordination Chemistry', Interscience, New York, 1960.
39. W. J. Geary, *Coord. Chem. Rev.* **1971**, *7*, 81.
40. N. N. Greenwood, B. P. Straughan, A. E. Wilson, *J. Chem. Soc. A: Inorg. Phys. Theo*. **1968**, 2209.
41. A. Sethukumar, C. Udhaya Kumar, R. Agilandeshwari, B. Arul Prakasam, *J. Mol. Struct.* **2013**, *1047*, 237.
42. D. C. Ilies, E. Pahontu, S. Shova, R. Georgescu, N. Stanica, R. Olar, A. Gulea, T. Rosu, *Polyhedron* **2014**, *81*, 123.
43. M. S. Refat, I. M. El-Deen, Z. M. Anwer, S. El-Ghol, *J. Mol. Struct.* **2009**, *920*, 149.
44. S. Chandra, S. Bargujar, R. Nirwal, N. Yadav, *Spectrochim. Acta Part A Mol. Biomol. Spectrosc.* **2013**, *106*, 91.
45. A. Sethukumar, C. Udhaya Kumar, R. Agilandeshwari, B. Arul Prakasam, *J. Mol. Struct.* **2013**, *1047*, 237.
46. T. S. Lobana, S. Indoria, M. Sharma, J. Nandi, A. K. Jassal, M. S. Hundal, A. Castineiras, *Polyhedron* **2014**, *80*, 34.
47. B. Şen, H. K. Kalhan, V. Demir, E. E. Güler, H. A. Kayalı, E. Subaşı, *Materials Science and Engineering: C* **2019**, *98*, 550.
48. R. Manikandan, P. Anitha, G. Prakash, P. Vijayan, P. Viswanathamurthi, R. J. Butcher, J. G. Malecki, *J. Mol. Catal. A Chem.* **2015**, *398*, 312.
49. S. A. Hosseini-Yazdi, S. Hosseinpour, A. A. Khandar, W. S. Kassel, N. A. Piro, *Inorg. Chim. Acta* **2015**, *427*, 124.
50. S. A. Hosseini-Yazdi, S. Hosseinpour, A. A. Khandar, J. White, *Transition Met. Chem.* **2016**, *41*, 65.
51. R. Venugopal, S. S. Sreejith, M. R. P. Kurup, *Polyhedron* **2019**, *158*, 398.
52. A. A. A. Abou-Hussein, W. Linert, *Spectrochim. Acta Part A Mol. Biomol. Spectrosc.* **2012**, *95*, 596.
53. Z. H. A. El-Wahab, M. M. Mashaly, A. A. Salman, B. A. El-Shetary, A. A. Faheim, *Spectrochim. Acta Part A Mol. Biomol. Spectrosc.* **2004**, *60*, 2861.
54. N. M. Rageh, A. M. A. Mawgoud, H. M. Mostafa, *Chem. Pap.* **1999**, *53*, 107.
55. R. Gup, B. Kirkan, *Spectrochim. Acta Part A Mol. Biomol. Spectrosc.* **2005**, *62*, 1188.
56. Mannar R. Maurya, S. Agarwal, C. Bader, D. Rehder, *Eur. J. Inorg. Chem.* **2005**, 147.
57. A. B. P. Lever, 'Inorganic electronic spectroscopy', Elsevier science, Amsterdam 1984.
58. D. N. Sathyanarayana, 'Electronic Absorption Spectroscopy and Related Techniques', Universities Press, 2001.
59. M. Gaber, H. A. El-Ghamry, M. A. Mansour, *J. Photochem. Photobiol. A* **2018**, *354*, 163.
60. S. A. AbouEl-Enein, S. M. Emam, M. W. Polis, E. M. Emara, *J. Mol. Struct.* **2015**, *1099*, 567.
61. S. M. Emam, S. A. Abouel-Enein, E. M. Abdel-Satar, *Appl. Organometal. Chem.* **2019**, *0*, e4847.
62. S. Chandra, K. Gupta, Sangeetika, *Synth. React. Inorg. Met-Org. Chem.* **2002**, *32*, 545.
63. M. Ali, A. Edwards, J. Tuah, M. Hossain, M. Nazimuddin, *Transition Metal Chemistry $V 23* **2004**, 41.
64. M. S. Chandra, *Open J. Inorg. Chem.* **2012**, *2*, 41.
65. S. Chandra, M. Tyagi, *J. Serb. Chem. Soc.* **2008**, *73*, 727.
66. S. Chandra, S. Raizada, S. Rani, *Spectrochim. Acta Part A Mol. Biomol. Spectrosc.* **2008**, *71*, 720.
67. M. F. R. Fouda, M. M. Abd-Elzaher, M. M. Shakdofa, F. A. El-Saied, M. I. Ayad, A. S. El Tabl, *J. Coord. Chem.* **2008**, *61*, 1983.
68. M. F. R. Fouda, M. M. Abd-Elzaher, M. M. E. Shakdofa, F. A. El Saied, M. I. Ayad, A. S. El Tabl, *Transition Met. Chem.* **2008**, *33*, 219.